Effect of size polydispersity on the structural and vibrational characteristics of two-dimensional granular assemblies*

Zhang Guo-Hua(张国华)[a)†], Sun Qi-Cheng(孙其诚)[b)], Shi Zhi-Ping(石志萍)[a)], Feng Xu(冯 旭)[a)], Gu Qiang(顾 强)[a)], and Jin Feng(金 峰)[b)]

[a)] *Department of Physics, University of Science and Technology Beijing, Beijing* 100083, *China*
[b)] *State Key Laboratory for Hydroscience and Engineering, Tsinghua University, Beijing* 100084, *China*

(Received 12 November 2013; revised manuscript received 12 March 2014; published online 15 May 2014)

Two-dimensional disordered granular assemblies composed of 2048 polydispersed frictionless disks are simulated using the discrete element method. The height of the first peak of the pair correlation function, g_1, the local and global bond orientational parameters $\psi_6^{\rm l}$ and $\psi_6^{\rm g}$, and the fluctuations of these parameters decrease with increasing polydispersity s, implying the transition from a polycrystalline state to an amorphous state in the system. As s increases, the peak position of the boson peak $\omega_{\rm BP}$ shifts towards a lower frequency and the intensity of the boson peak $D(\omega_{\rm BP})/\omega_{\rm BP}$ increases, indicating that the position and the strength of the boson peak are controlled by the polydispersity of the system. Moreover, the inverse of the boson peak intensity $\omega_{\rm BP}/D(\omega_{\rm BP})$, the shear modulus G, and the basin curvature $S_{\rm IS}$ all have a similar dependence on s, implying that the s dependence of the vibrational density of states at low frequencies likely originates from the s dependence of the basin curvature.

Keywords: granular matter, vibrational characteristics, size polydispersity, structural characteristics

PACS: 63.50.–x, 45.70.–n, 61.43.–j **DOI:** 10.1088/1674-1056/23/7/076301

1. Introduction

The vibrational density of states (VDOS) of amorphous materials, such as molecular glass and granular media, differs from that of crystalline materials due to the absence of a long-range positional order. The usual Debye behavior $D(\omega) \propto \omega^{d-1}$ is expected for the low frequency part of the vibrational spectrum in crystals, where ω is the frequency of the normal modes and d is the number of dimensions of the crystal. In contrast, excess low-frequency modes appear in the VDOS of disordered solids when compared to a typical Debye response.[1–3] This behavior is identified in the reduced VDOS spectrum (i.e., $D(\omega)$ vs. ω^{d-1}), which shows a boson peak at low frequencies.

One feature of the density of states of jammed disordered solids is that a plateau appears in the low frequency.[1] An interesting observation is that the plateau extends to a lower frequency when $\Delta\phi$ ($\Delta\phi \equiv \phi - \phi_{\rm c}$, where $\phi_{\rm c}$ is the packing fraction of point J) decreases. The characteristic frequency ω^*, below which $D(\omega)$ quickly decreases to zero, scales according to $\omega^* \sim (\Delta\phi)^{1/2}$ for the system with a harmonic repulsion.[2,3] The characteristic length scale ξ, which can be determined from the dominant wave vector contributing to the eigenmode at ω^*, diverges as a power law in $\Delta\phi$. Below ξ the system behaves like a marginal solid at point J, while above ξ the system behaves like an ordinary elastic solid.[4,5]

An effective approach to obtaining information on the nature of the boson peak of a disordered system is to study its evolution as a function of the control parameters, such as temperature and load. Recently, significant research attention has been focused on the parameter dependence of the frequency $\omega_{\rm BP}$ and the intensity $I_{\rm BP}$ of the boson peak of disordered systems. Three common opinions have arisen: (i) as the applied pressure or density increases, $\omega_{\rm BP}$ simultaneously increases while $I_{\rm BP}$ decreases;[6–8] (ii) the rescaled $D(\omega)$ can be obtained by normalizing the frequency by $\omega_{\rm BP}$ and the VDOS by $I_{\rm BP}$,[9] which remains invariant with respect to the applied pressure in the proximity of the boson peak; and, (iii) the height of the boson peak is inversely proportional to the shear modulus in a two-dimensional frictionless athermal sphere packing.[10]

A different competing hypothesis has been proposed to explain the nature of the vibrational modes at low frequencies for disordered systems. Some authors attribute the boson peak to local[11,12] or quasi-local vibrations.[13,14] Others attribute the peak to the acoustic Van Hove singularity in crystals, which shifts to a lower energy due to the force-constant disorder.[15,16] Léonforte attributed the boson peak anomaly of the density of states to physics on scales below which the classical homogeneous continuum elastic theories must necessarily break down.[17] Rufflé suggested that the boson peak frequency is closely related to the Ioffe–Regel limit for sound in many glasses.[18] However, the origin of the boson peak remains a puzzle, and there is a lack of experiments and simu-

*Project supported by the National Natural Science Foundation of China (Grant Nos. 11272048, 51239006, and 11034010), the European Commission Marie Curie Actions (Grant No. IRSES-294976), and the National Basic Research Program of China (Grant No. 2010CB731504).

†Corresponding author. E-mail: zhguohua@sas.ustb.edu.cn

© 2014 Chinese Physical Society and IOP Publishing Ltd

lations focused on the nature of $D(\omega)$ at low frequencies.

Granular materials in nature and industry consist of particles with different size polydispersity. In addition, polydispersity has a significant effect on both the structure and the dynamics of granular systems.[19] For example, increasing polydispersity at a fixed volume fraction lowers the structural correlation, pressure, energy, and viscosity of colloidal systems. Polydispersity in most studies, so far, has been restricted to narrow size distributions mainly to prevent the long-range structural order and bidispersity; however, there are a few studies where broader ranges of particle-size distributions are investigated. In this paper, we focus on the effect of size polydispersity on the structural and the vibrational characteristics of two-dimensional (2D) granular assemblies. Polydispersed 2D disordered granular ensembles are generated using the discrete element method, with each ensemble possessing 100 independent initial configurations under a fixed pressure. An analysis of the system covers the vibrational density of states of the granular ensembles, the effect of polydispersity on the pair correlation function, the bond orientational order, the frequency and the intensity of the boson peak, the participation ratio, the basin curvature, and the shear modulus of the system.

2. Numerical details

A two-dimensional disordered granular system composed of 2048 polydispersed frictionless disks is generated within a square periodic cell of length L. In order to vary the degree of the polydispersed size, the mass and the stiffness of each disk is fixed, while the disk diameters are polydispersed with a uniform distribution between $d_0(1-s/2)$ and $d_0(1+s/2)$, where s is the size polydispersity. In this paper, all particles have the same mass, and s ranges from 0 to 0.5. The disks interact through a finite-range, purely repulsive linear spring potential

$$V_{ij} = \frac{1}{2}\varepsilon_{ij}(1-r_{ij}/\sigma_{ij})^2\Theta(1-r_{ij}/\sigma_{ij}), \tag{1}$$

where r_{ij} is the center to center separation between particles i and j, $\sigma_{ij} = r_i + r_j$ is the average diameter of the two particles, r_i and r_j are the radii of particles i and j, respectively, and $\Theta(x)$ is the Heaviside function. The variable ε_{ij} is the characteristic energy of the interaction,[20] $\varepsilon_{ij} = k_i k_j (r_i + r_j)^2/(k_i + k_j)$, where k_i and k_j are the normal stiffness of particles i and j, respectively. The repulsive linear spring model is used in our simulation because the packing studied here is composed of 2D disks instead of spheres where the attractive force can be neglected.

The $T = 0$ configurations at a given pressure p are generated through the following protocol. First, N particles are randomly generated in a square periodical box at a given packing fraction (corresponding to a $T = \infty$ configuration). Next, the $T = \infty$ configuration is relaxed to a metastable state with local energy minimum (corresponding to a $T = 0$ configuration). The particle diameters are then successively changed until the pressure of the system approximates the target pressure. Here, 100 different configurations are generated for each polydispersity value.

The vibrational mode and its density of state can be obtained by solving the secular equation

$$|\boldsymbol{F} - \omega^2 \boldsymbol{I}| = 0, \tag{2}$$

where $\boldsymbol{F}$ is the mass weighted Hessian matrix, $F_{ij} = H_{ij}/\sqrt{m_i m_j}$, $H_{ij} = \partial^2 V/\partial R_i \partial R_j$, m_i and m_j are the masses of particles i and j, respectively, and R_i and R_j are the coordinates (x or y) of particles i and j, respectively. It is worth noting that using the repulsive linear spring potential will introduce a discontinuity in H_{ij}, and make the jammed particulate system inherently nonharmonic as $\Delta\phi \to 0$.[21]

A set of eigenvalues and the corresponding eigenvectors of Eq. (2) can be obtained by diagonalizing the Hessian matrix for each stable configuration, where the eigenvalue is the square of the vibrational frequency ω^2 and the eigenvector is the displacement vector of the corresponding normal mode. All of the densities of vibrational states are averaged over the 100 configurations at a fixed pressure ($p = 2 \times 10^{-3}$) for each polydispersity value. We use the mean diameter $\bar{\sigma}$, m, and $(m\bar{\sigma}^2/\varepsilon)^{1/2}$ as the units of length, mass, and time, respectively.

3. Results and discussion

3.1. Evolution of structural characteristics

The pair correlation function $g(r)$ is an effective tool for studying the structural properties of disordered materials.[22] Figure 1 shows $g(r)$ at $s = 0.001$, 0.005, 0.008, 0.02, 0.1, 0.2, 0.3, 0.4, 0.5, respectively. The s dependence of the height of the first peak of $g(r)$, g_1, is plotted in the inset of Fig. 1. The strong first peak, the split of the second peak, and the existence of peaks at large r for configurations where $s < 0.1$ indicate that there is a long-range order phase in these configurations.

When $s > 0.1$, the first peak of $g(r)$ is broadened, its height decays faster with r as s increases, and the first two peaks are no longer distinguishable, which indicates that the long range order of the system disappears. This implies that there is a crossover polydispersity ($s^* \sim 0.1$) from a polycrystalline state to an amorphous state as polydispersity increases. This result is mirrored in the evolution of the relationship between the bond orientational order parameter and s, see Fig. 2.

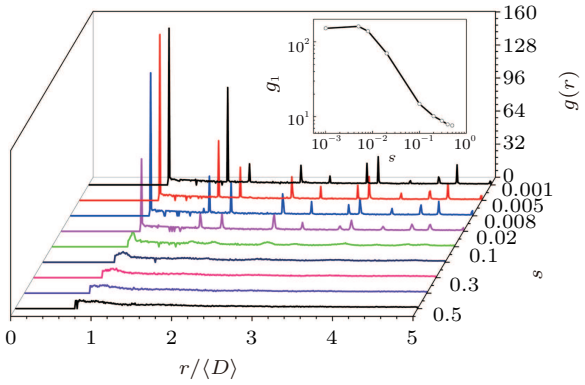


Fig. 1. (color online) Pair-correlation function $g(r)$ at $s = 0.001$, 0.005, 0.008, 0.02, 0.1, 0.2, 0.3, 0.4, 0.5, respectively. Inset shows the height of the first peak of $g(r)$, g_1, as a function of s.

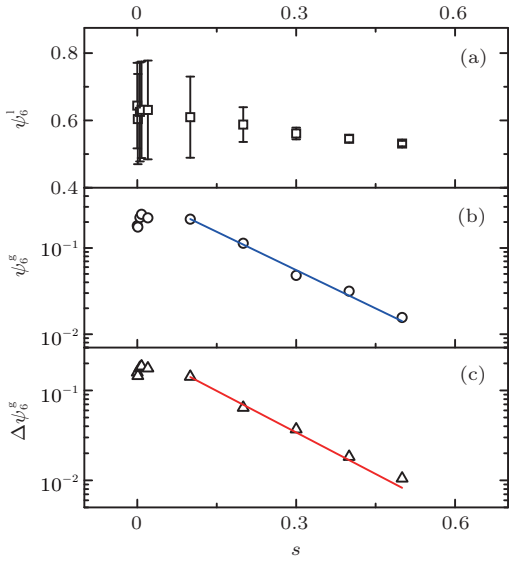


Fig. 2. (color online) (a) Local ψ_6^l (open square) and (b) global ψ_6^g (open circle) versus polydispersity s. The error bars represent the standard deviation over 100 configurations. (c) Standard deviation of ψ_6^g versus s. The lines in panels (b) and (c) are exponential fits of ψ_6^g and $\Delta\psi_6^g$ for $s > 0.1$.

The bond orientational order parameter ψ_6 quantifies the positional order of the configuration measuring the hexagonal registry of nearest neighbors.[23,24] The global bond-orientational order parameter ψ_6^g for a (sub-)system of linear dimension L is simply the absolute value of the average over all particles, and the local bond orientational order parameter ψ_6^l does not consider the phase information. Here ψ_6^g and ψ_6^l are defined as

$$\psi_6^g = \frac{1}{N}\left|\sum_{k=1}^{N}\frac{1}{n_k}\sum_{j=1}^{n_k} e^{i6\theta_{kj}}\right|, \quad \psi_6^l = \frac{1}{N}\sum_{k=1}^{N}\frac{1}{n_k}\left|\sum_{j=1}^{n_k} e^{i6\theta_{kj}}\right|, \quad (3)$$

where N is the number of particles in the (sub-)system, the sum on j runs over all n_k neighbors of this particle, and θ_{kj} is the angle between a central particle k and a neighbor j and an arbitrary but fixed reference axis. Two particles are considered neighbors if the center to center distance $r_{ij} < r_{\min}\sigma_{ij}$, where $r_{\min}$ is set as the first minimum of $g(r)$ in the system. Note that $\psi_6^g = 1$ indicates a perfect hexagonal arrangement with six nearest neighbors, while $\psi_6^g = 0$ indicates a totally random arrangement. For a polycrystal, the global order parameter is $\psi_6^g \propto 1/\sqrt{N_d}$, where N_d is the number of polycrystalline domains.

Figures 2(a) and 2(b) show ψ_6^l and ψ_6^g, respectively, as a function of the polydispersity. The error bars in Fig. 2(a) represent the standard deviation of ψ_6^l over the 100 different configurations. The figure shows that ψ_6^g is smaller than ψ_6^l for the entire range of s because of the orientational difference between the ordered domains, and there is a strong correlation between s and the local and global bond orientational orders. Both ψ_6^l and ψ_6^g decrease with increasing s, that is, structures with a smaller s typically have larger values of ψ_6^g and so exhibit more order. At smaller values of s ($s < 0.1$), $\psi_6^l = 0.63$ and $\psi_6^g = 0.25$, implying that few polycrystalline domains ($\langle N_d\rangle \sim 16$) exist in each configuration. Alternatively, when $\psi_6^g = 0$ and $\psi_6^l = 0.53$, s is larger than 0.2, which is close to $\psi_6^l = 0.55$ found in dense liquids.[24] This result is consistent with the equilibrium phase behavior of polydispersed hard spheres, where beyond a terminal polydispersity of 0.12, crystallization does not occur.[25]

The dependence on s of the standard deviation of ψ_6^g is shown in Fig. 2(c), where the fluctuations in both ψ_6^g and ψ_6^l decrease as s increases. The large fluctuation of ψ_6^g when s is smaller than 0.1 means that there is a large difference in the number of ordered domains with different orientations between configurations with the same polydispersity. The fluctuation of ψ_6^g decays exponentially as s increases, which means that configurations with larger values of s are more homogeneous. This may be due to the increasing number of ordered domains with the increase of s, as mentioned above.

3.2. Vibrational density of states

The vibrational densities of states for polydispersed granular packings composed of 2048 particles with $s = 0.001$, 0.005, 0.008, 0.02, 0.1 are shown in Fig. 3. Two strong peaks at $\omega = 1.4$ and $\omega = 2.2$ appear in the $D(\omega) \sim \omega$ curve when s equals 0.001, which we associate with the crystallization in the system.[23] Note that the two peaks gradually disappear as s increases, implying that the system becomes more amorphous when s increases. Furthermore, the $D(\omega) \sim \omega$ curves almost collapse upon one another for s larger than 0.1 (the curves are not shown in this paper), which means that the system is highly amorphous when s is larger than 0.1. The weight of the low frequency portion of each peak of the $D(\omega) \sim \omega$ curve (i.e., when $\omega < 1.0$) increases as s increases, while the weight of the high frequency portion of each peak of the $D(\omega) \sim \omega$ curve (i.e., $1.0 < \omega < 1.5$ and $\omega > 2.1$) decreases. This result indicates that increasing the degree of disorder increases the number of soft modes in the system.

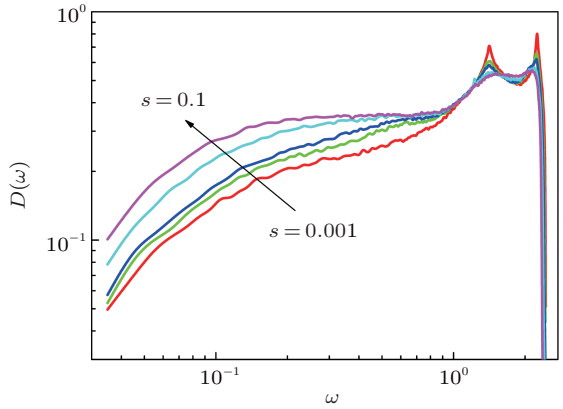


Fig. 3. (color online) Density of states as a function of ω for systems with different size polydispersity, here $s = 0.001$, 0.005, 0.008, 0.02, 0.1 (from bottom to top). The scaled angular frequency is given by $\omega = 2\pi\nu\sqrt{m\overline{\sigma}^2/\varepsilon}$, where ν is the frequency.

3.3. Participation ratio

The participation ratio gives information on the number of particles participating in a given mode; that is, it is a measure of the extensiveness of a mode

$$P_{\mathrm{R}}(\omega_n) = \frac{1}{N}\frac{\sum_i |e_{n,i}|^2}{\sum_i |e_{n,i}|^4}, \tag{4}$$

where $e_{n,i}$ is the polarization vector of particle i in mode n with frequency ω_n, and the sum runs over all particles in the system except for the rattlers. In general, P_{R} ranges from 0 to 1, where P_{R} is of the order of $1/N$ for the localized modes and is of the order of 1 for the extended modes. Figure 4 depicts the typical eigenmodes with different participation ratios for a configuration with $s = 0.1$. At low frequencies, the eigenmodes have a small P_{R}, which are quasilocalized with the localized structure superimposed on a plane-wave-like background, as shown in Fig. 4(a). At intermediate frequencies, the eigenmodes are highly disordered and extended, see Fig. 4(b). At high frequencies, the modes are localized (Fig. 4(c)).

The plot of P_{R} in Fig. 5 shows the localization properties of the normal modes. Three characteristics are apparent in the $P_{\mathrm{R}}(\omega) \sim \omega$ curves for $s = 0.001$, 0.005, 0.008, 0.02, 0.1. (i) The participation ratio of the modes is lower than 0.1 at the high frequency and lower than 0.2 at the low frequency, which indicates that the modes at the high frequency end of the spectrum are localized and there are quasilocalized modes in the low frequency region for a given configuration. This result is consist with the results from the previous studies.[26] (ii) There is a crossover frequency ω^+ (≈ 0.5) in the $P_{\mathrm{R}}(\omega) \sim \omega$ curves for $s = 0.001$, 0.005, 0.008, 0.02, 0.1. The $P_{\mathrm{R}}(\omega)$ decreases with s increasing since ω is larger than ω^+, meaning that the system can not sustain the propagating mode as the size polydispersity increases. This is very similar to the $P_{\mathrm{R}}(\omega) \sim \omega$ curve of a supercooled polydispersed liquid.[27] While $P_{\mathrm{R}}(\omega)$ increases with increasing s when ω is smaller than ω^+, it also suggests that the size disorder can decrease the degree of localization in low frequency modes ($\omega < \omega^+$). (iii) The $P_{\mathrm{R}}(\omega)$ in the whole region of ω never exceeds 0.4, which indicates that the system is still very heterogeneous on the length scale of the simulation box. A similar result has been obtained in a soft colloidal glass[9] and in a model glass.[28,29]

3.4. Boson peak

The curves of the reduced density of states, $D(\omega)/\omega$ vs. ω, are plotted in Fig. 6 for $s = 0.001$, 0.005, 0.008, 0.02, 0.1. All of the reduced densities of states $D(\omega)/\omega$ have a peak at approximately $\omega = 0.08$, which contrasts with the prediction of the Debye model; that is, $D(\omega) \propto \omega^{d-1}$. The peak position of the boson peak ω_{BP} shifts towards a lower frequency, and the intensity of the boson peak $D(\omega_{\mathrm{BP}})/\omega_{\mathrm{BP}}$ becomes stronger as s increases. This means that both the position and the strength of the boson peak of a granular system are controlled by the polydispersity. The s dependence of $D(\omega_{\mathrm{BP}})/\omega_{\mathrm{BP}}$ is shown in Fig. 7(a). Again, the dependence on s for $D(\omega_{\mathrm{BP}})/\omega_{\mathrm{BP}}$ is different for large and small values of s; when s is less than 0.1, $D(\omega_{\mathrm{BP}})/\omega_{\mathrm{BP}}$ increases rapidly with increasing s, while $D(\omega_{\mathrm{BP}})/\omega_{\mathrm{BP}}$ shows virtually no change until s is equal to 0.5. The boson peak frequency ω_{BP} has a weaker s dependence than that of $D(\omega_{\mathrm{BP}})/\omega_{\mathrm{BP}}$, and the dependence of $D(\omega)/\omega$ on s versus the dependence of the ω spectrum on the polydispersity implies that the size disorder is an important factor behind the boson peak. Note that a similar result has been reported on the VDOS of supercooled polydispersed liquids.[19]

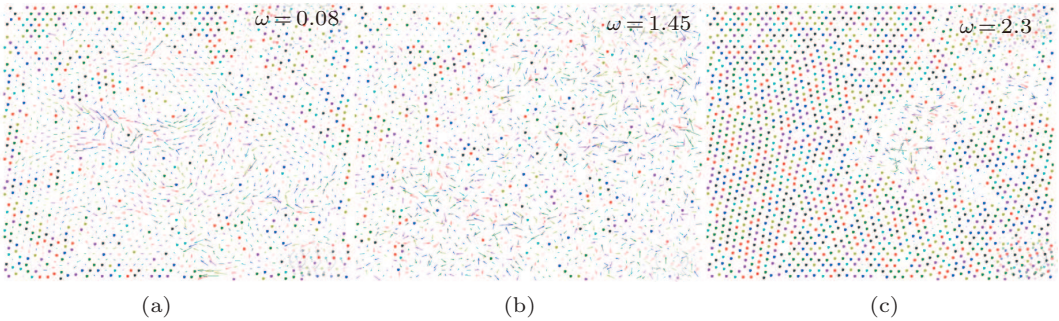


Fig. 4. (color online) Eigenmodes at (a) low frequency, (b) intermediate frequency, and (c) high frequency for a configuration with $s = 0.1$.

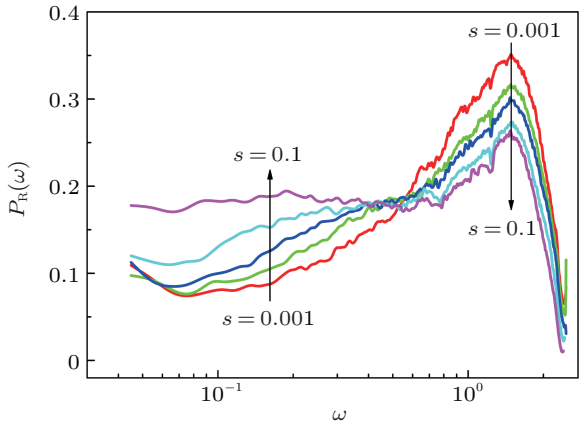


Fig. 5. (color online) Participation ratio versus normalized frequencies of the normal modes for various size polydispersity. The size polydispersity from bottom to top is $s = 0.001$, 0.005, 0.008, 0.02, 0.1 when ω is smaller than 0.5, and it is just the reverse when ω is larger than 0.5.

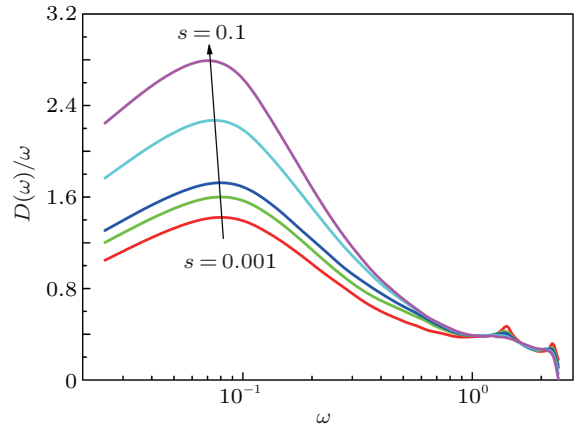


Fig. 6. (color online) Reduced density of states $D(\omega)/\omega$ of a 2D system under constant pressure $p = 2 \times 10^{-3}$ plotted as a function of frequency ω. From bottom to top, $s = 0.001$, 0.005, 0.008, 0.02, 0.1.

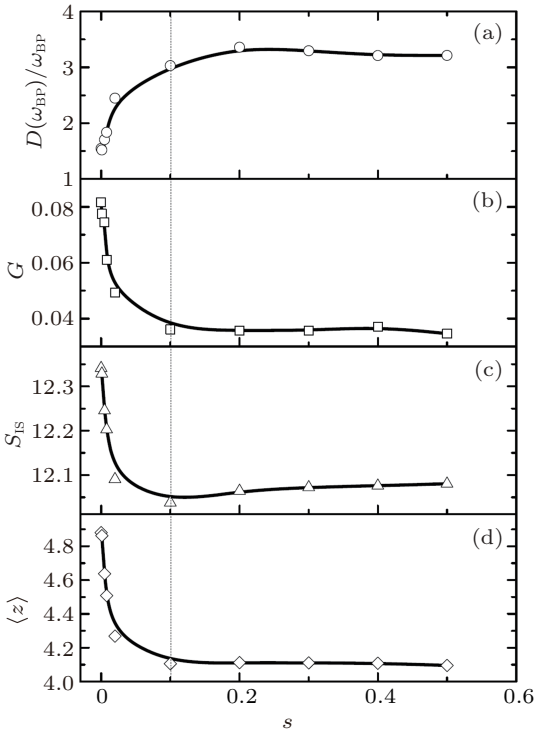


Fig. 7. The s dependence of: (a) boson peak intensity $D(\omega_{BP})/\omega_{BP}$, (b) shear modulus G, (c) basin curvature S_{IS}, and (d) average coordination number $\langle z \rangle$.

The boson peak amplitude is inversely proportional to the shear modulus G for a 2D glass system.[10] We study this relationship in a 2D athermal frictionless granular system. The static linear shear modulus G of the system is measured using a standard method. First, an infinitesimal simple shear strain $d\gamma$, which is less than 10^{-7}, is applied to deform the system, then the system is relaxed to the metastable state with local energy minimum. The resulting shear stress $d\Sigma_{xy}$ is measured, and the shear modulus G of the system is obtained, where $G = d\Sigma_{xy}/d\gamma$. Each shear modulus is obtained by averaging over the 100 configurations with the same polydispersity. The plot of shear modulus versus degree of size polydispersity is given in Fig. 7(b), which shows G decreasing rapidly as s increases up to a value of 0.1, then remaining constant. The inverse of the height of the boson peak $\omega_{BP}/D(\omega_{BP})$ versus shear modulus G is plotted in Fig. 8. The inverse of the height of the boson peak $\omega_{BP}/D(\omega_{BP})$ is proportional to the shear modulus G

$$\frac{D(\omega_{BP})}{\omega_{BP}} \propto \frac{1}{K} + \frac{1}{G} \approx \frac{1}{G}, \tag{5}$$

because the bulk modulus K of a granular assembly is about 4 or 5 times the shear modulus. Equation (5) shows that the boson peak amplitude is inversely proportional to G, which indicates that the density of excess modes caused by the size disorder should give a significant contribution to the shear modulus. This result is consistent with that of glass systems,[9,10,26] where the excess modes are associated with the lowest energy barriers for rearrangements, and have important consequences for the system stability.

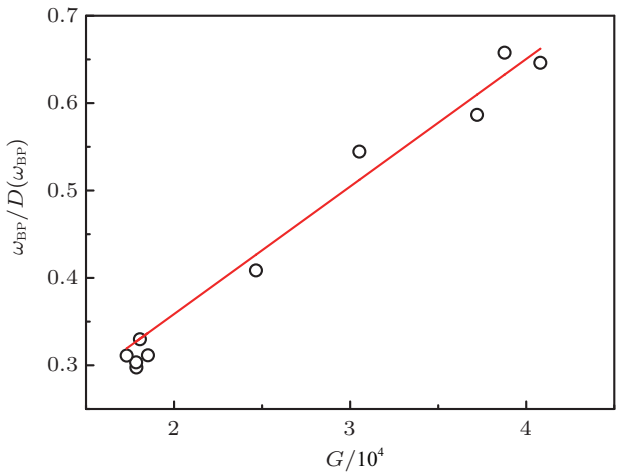


Fig. 8. (color online) Inverse of the height of the boson peak $\omega_{BP}/D(\omega_{BP})$ versus shear modulus G. The line is a linear fit.

3.5. Basin curvature

One approach to understanding the complex dynamics of a granular assembly is to consider the influence of the system's potential energy landscape (PEL) on its relaxation processes.[30] In the PEL, each configuration of inherent structures is characterized by its potential energy and pressure, and

by the dN local curvatures of the PEL. We can view the dynamics of the system as the motion of the state point in the dN-dimensional configuration space, where N is the number of particles. In general, we can separate the trajectories in the configuration space into intrabasin and interbasin components. The intrabasin motion has been associated with the high frequency vibrational dynamics, while the structural relaxation may be related to the process of exploration of different basins. One possible measure of the average basin curvature is the shape function[31]

$$S_{\rm IS} = \frac{1}{N}\sum_{i=1}^{2N-2}\log(\omega_i), \tag{6}$$

where ω_i is the frequency of vibrational mode i. Note that $S_{\rm IS}$ is very sensitive to the spectrum tails because of the summation of logarithms.[32]

In Fig. 7(c), we plot the basin curvature $S_{\rm IS}$ as a function of s, where each $S_{\rm IS}$ is averaged over 100 configurations using the same polydispersity and pressure. The configurations with smaller s have larger $S_{\rm IS}$, indicating that the higher polydispersity configurations with larger s have flatter basins. This is consistent with the results found in jammed solids[26] and supercooled liquids.[19] It is worth noticing that $\omega_{\rm BP}/D(\omega_{\rm BP})$, G, and $S_{\rm IS}$ exhibit a similar dependence on s; in other words, these variables change synchronously as s changes. For example, the variables rapidly decrease in a synchronous fashion as s increases when $s < 0.1$, then become constant for s greater than 0.1, as mentioned above. Therefore, we can reasonably infer that the s dependence of the VDOS at low frequencies most likely originates from the s dependence of the basin curvature.

It is worth mentioning that the effects of s on the peak of $D(\omega_{\rm BP})/\omega_{\rm BP}$, G, and $S_{\rm IS}$ are not strong. As s increases 100 times from 0.001 to 0.1, the intensity of the peak and G both change by a factor of 2. In order to understand the s dependences of $D(\omega_{\rm BP})/\omega_{\rm BP}$ and G, the average coordination number $\langle z\rangle$ (the average number of contacts per particle) is calculated. Figure 7(d) shows $\langle z\rangle$ as a function of s, where each $\langle z\rangle$ is averaged over the 100 configurations with the same polydispersity and pressure. As shown in Fig. 7(d), $\langle z\rangle$ has a similar s dependence with $\omega_{\rm BP}/D(\omega_{\rm BP})$, G, and $S_{\rm IS}$. Figure 7 suggests that increasing the size polydispersity at a given pressure would lead to the reduction of the constraint number, and the appearance of the boson peak is a consequence of the reduction of constraints in an overconstrained packing, which is consistent with the prediction of the perturbation theory.[33] The effects of s on the peak of $D(\omega_{\rm BP})/\omega_{\rm BP}$, G, and $S_{\rm IS}$ being not strong may be due to the fact that $\langle z\rangle$ is only changed by 20% (decreases from 4.9 to 4.1) when s increases from 0.001 to 0.1. The fact that G decreases by a factor of two whereas $S_{\rm IS}$ only changes less than 2% as s increases 100 times from 0.001 to 0.1 implies that at higher polydispersity the system has smaller barriers to diffusion and it also has more relaxation channels available.

4. Conclusion

The present work reports an investigation of the effect of polydispersity on the structural and the vibrational properties of a two-dimensional, frictionless granular packing prepared by a quenching procedure of the discrete element method. The height of the first peak of $g(r)$, g_1, the local and global bond orientational parameters $\psi_6^{\rm l}$ and $\psi_6^{\rm g}$, and their fluctuations all decrease with increasing polydispersity s, implying that the system transits from a polycrystalline state to an amorphous state as polydispersity increases.

The normal modes of the system are obtained by diagonalizing the Hessian matrix for each stable configuration with the same s, and the harmonic vibrational properties are investigated in detail. The weight of the low frequency portion of each peak of the $D(\omega)\sim\omega$ curves increases with increasing s, implying that increasing the degree of disorder of the system enhances the number of the soft modes. There is a crossover frequency ω^{+} (≈ 0.5) in the $P_{\rm R}(\omega)\sim\omega$ curves for all the s values studied, above which the value of $P_{\rm R}(\omega)$ decreases as s increases, meaning that the system can not sustain the propagating mode as the size polydispersity increases.

The reduced density of states exhibits a boson peak feature. The peak position of the boson peak $\omega_{\rm BP}$ shifts towards a lower frequency and the intensity of the boson peak $D(\omega_{\rm BP})/\omega_{\rm BP}$ becomes stronger as s increases, implying that the position and the strength of the boson peak of a granular system are controlled by the polydispersity of the system. The basin curvature $S_{\rm IS}$ and the shear modulus G are also functions of the system's polydispersity. We find that the boson peak amplitude is inversely proportional to the shear modulus G, as is found in a 2D glass system. Moreover, $\omega_{\rm BP}/D(\omega_{\rm BP})$, G, and $S_{\rm IS}$ all show a similar dependence on s, implying that the s dependence of the VDOS at low frequencies probably originates from the s dependence of the basin curvature.

Acknowledgment

We are grateful to N. Xu for helpful discussion.

References

[1] O'Hern C S, Silbert L E and Nagel S R 2003 *Phys. Rev. E* **68** 011306
[2] Silbert L E, Liu A J and Nagel S R 2005 *Phys. Rev. Lett.* **95** 098301
[3] Wyart M, Nagel S R and Witten T A 2005 *Europhys. Lett.* **72** 486
[4] Silbert L E, Liu A J and Nagel S R 2009 *Phys. Rev. E* **79** 021308
[5] Wyart M, Silbert L and Nagel S 2005 *Phys. Rev. E* **72** 051306
[6] Stavrou E, Raptis C and Syassen K 2010 *Phys. Rev. B* **81** 174202
[7] Srivastava D and Sarkar S K 2012 *Phys. Rev. B* **85** 024206
[8] Gurevich V L, Parshin D A and Schober H R 2005 *Phys. Rev. B* **71** 014209

[9] Chen K, Ellenbroek W G, Zhang Z, Chen D T, Yunker P J, Henkes S, Brito C, Dauchot O, van Saarloos W, Liu A J and Yodh A G 2010 *Phys. Rev. Lett.* **105** 025501

[10] Shintani H and Tanaka H 2008 *Nat. Mater.* **7** 870

[11] Laird B and Schober H 1991 *Phys. Rev. Lett.* **66** 636

[12] Schober H R and Oligschleger C 1996 *Phys. Rev. B* **53** 11469

[13] Rufflé B, Parshin D A, Courtens E and Vacher R 2008 *Phys. Rev. Lett.* **100** 015501

[14] Tanguy A, Wittmer J P, Leonforte F and Barrat J L 2002 *Phys. Rev. B* **66** 174205

[15] Chumakov A I, Monaco G, Monaco A, Crichton W A, Bosak A, Rüffer R, Meyer A, Kargl F, Comez L, Fioretto D, Giefers H, Roitsch S, Wortmann G, Manghnani M H, Hushur A, Williams Q, Balogh J, Parliński K, Jochym P and Piekarz P 2011 *Phys. Rev. Lett.* **106** 225501

[16] Schirmacher W, Diezemann G and Ganter C 1998 *Phys. Rev. Lett.* **81** 136

[17] Léonforte F, Tanguy A, Wittmer J P and Barrat J L 2006 *Phys. Rev. Lett.* **97** 055501

[18] Rufflé B, Guimbretière G, Courtens E, Vacher R and Monaco G 2006 *Phys. Rev. Lett.* **96** 045502

[19] Abraham S E, Bhattacharrya S M and Bagchi B 2008 *Phys. Rev. Lett.* **100** 167801

[20] Henkes S, Hecke M V and Saarloos W V 2010 *Europhys. Lett.* **90** 14003

[21] Schreck C F, Bertrand T, O'Hern C S and Shattuck M D 2011 *Phys. Rev. Lett.* **107** 078301

[22] Silbert L, Liu A and Nagel S 2006 *Phys. Rev. E* **73** 041304

[23] Schreck C F, O'Hern C S and Silbert L E 2011 *Phys. Rev. E* **84** 011305

[24] Steinhardt P J, Nelson D R and Ronchetti M 1983 *Phys. Rev. B* **28** 784

[25] Sollich P and Wilding N B 2010 *Phys. Rev. Lett.* **104** 118302

[26] Xu N, Vitelli V, Liu A J and Nagel S R 2010 *Europhys. Lett.* **90** 56001

[27] Abraham S E and Bagchi B 2010 *Phys. Rev. E* **81** 031506

[28] Rovigatti L, Kob W and Sciortino F 2011 *The Journal of Chemical Physics* **135** 104502

[29] Derlet P M, Maaβ R and Löffler J F 2012 *Euro. Phys. J. B* **85** 1

[30] Sastry S, Debenedetti P G and Stillinger F H 1998 *Nature* **393** 554

[31] Giovambattista N, Stanley H E and Sciortino F 2003 *Phys. Rev. Lett.* **91** 115504

[32] Mossa S, La Nave E, Stanley H E, Donati C, Sciortino F and Tartaglia P 2002 *Phys. Rev. E* **65** 041205

[33] Flores-Ruiz H M and Naumis G G 2011 *Phys. Rev. B* **83** 184204